

Continuous ion-selective separations by shock electro dialysis

Kameron M. Conforti¹  | Martin Z. Bazant^{1,2} 

¹Department of Chemical Engineering, Massachusetts Institute of Technology (MIT), Cambridge, Massachusetts

²Department of Mathematics, Massachusetts Institute of Technology (MIT), Cambridge, Massachusetts

Correspondence

Martin Z. Bazant, Department of Chemical Engineering and Department of Mathematics, Massachusetts Institute of Technology (MIT), Cambridge, MA.

Email: bazant@mit.edu

Funding information

Massachusetts Institute of Technology

Abstract

Water purification remains a challenge across sectors worldwide, especially the efficient removal of specific (toxic or valuable) dissolved ions at low salinity. In this article, shock electro dialysis (SED) is shown for the first time to have this capability, by demonstrating continuous separation of magnesium ions from aqueous mixtures of NaCl and MgCl₂. By systematically measuring the composition of all input and output streams, the mechanisms that drive selectivity, current efficiency, and desalination are revealed, as well as strategies to improve performance. For solutions initially rich in sodium, highly selective (> 98%) continuous removal of magnesium can be achieved with only moderate (50–70%) total salt removal. This remarkable selectivity is associated with super-diffusive ion transport, mediated by charged double layers in a porous glass frit, behind a steady deionization shockwave in cross flow.

KEYWORDS

deionization shockwaves, electrochemical transport, electrokinetics, overlimiting current, separation techniques, water treatment

1 | INTRODUCTION

According to the World Health Organization (WHO) and the United Nations International Children's Emergency Fund (UNICEF), 29% of the global population is not using a safely managed water source.¹ Eight percent of the world's population relies on surface water or another unimproved source; regionally, this fraction can soar beyond 40%.¹ Even in developed nations, such as the United States, degradation of local infrastructure can leave many without reliable access to clean drinking water, as illustrated by the recent case of Flint, Michigan, where residents faced dangerously high levels of lead in their water due to municipal pipe corrosion.^{2–4} As many toxic ions exist in their multivalent forms in water (e.g., Pb²⁺, HAsO₄^{2–}, and Cu²⁺), an efficient and continuous method for selective removal of multivalent ions would have tremendous impact on clean water availability and public health.

Shock electro dialysis (SED) is an emerging electrochemical method for water treatment^{5–7} exploiting deionization shockwaves in charged porous media.^{8,9} SED operates by passing a large over-limiting current (faster than diffusion) perpendicular to the pressure-driven flow of an electrolyte through a charged porous medium, placed between two ion-selective elements, such as membranes or electrodes. It is well known that over-

limiting current can be supported by electrokinetic and electrochemical phenomena in bulk electrolytes,¹⁰ but confinement in a charged pore or microchannel opens new surface-driven mechanisms for super-diffusive transport. In particular, surface conduction (SC) and electroosmotic flow (EOF) provide the system with overlimiting conductance^{11,12} and enable the propagation of a sharp deionization shock wave^{12–14} (or a steady ion-concentration polarization layer),^{15–17} which divides the fluid into depleted and enriched regions. Ions in the depleted region remain in electric double layers and electro-osmotic convection cells close to the oppositely charged walls, as the bulk fluid becomes deionized. These extreme, surface-driven ion transport phenomena also occur in charged porous media,^{8,9} where the current and flow directions can be decoupled and exploited for SED.⁷ In cross flow, the deionized fluid behind the shock can be collected separately from the rest of the electrolyte as shown in Figure 1a.

The time is ripe to investigate the ionic separation capabilities of SED, since previous work has only considered total desalination of binary electrolytes,^{7–9,18} while the theory predicts large gradients in electric field and salt concentration across the shock that could cause very different transport rates for specific ions. The first demonstrations of SED were performed in a batch copper electrodeposition cell, which

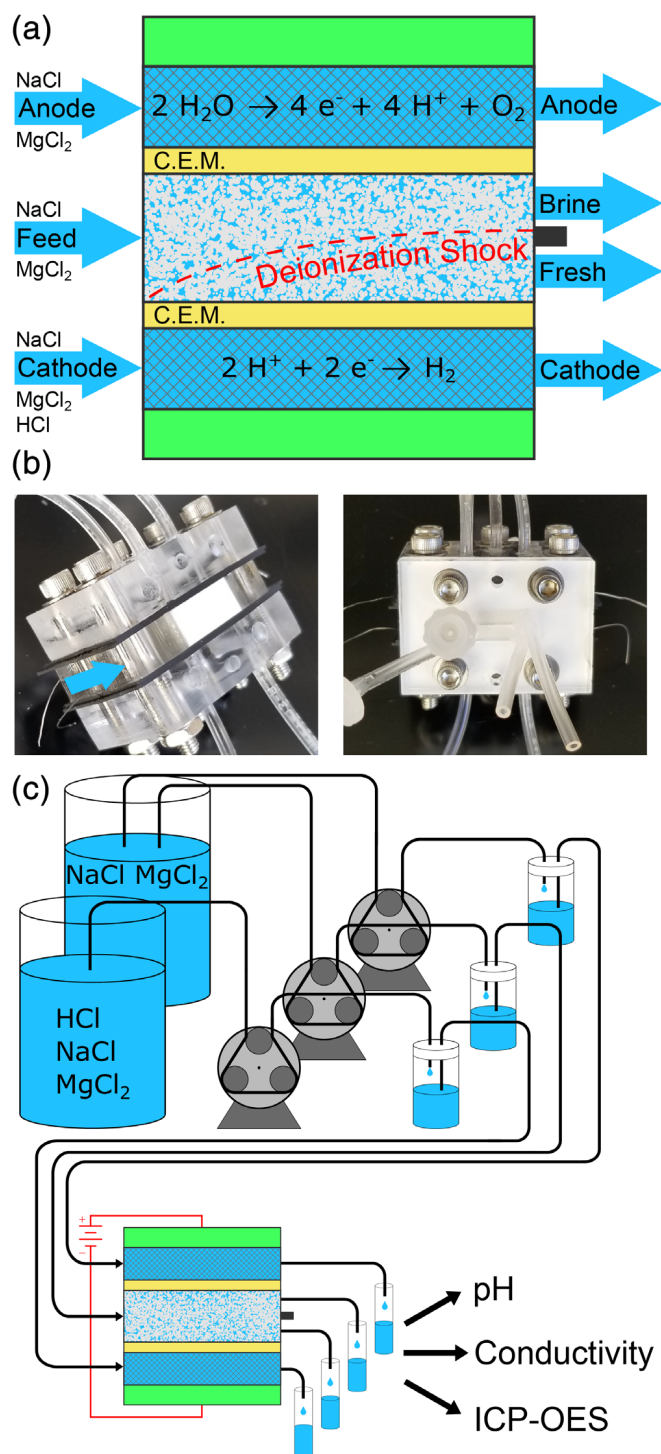


FIGURE 1 (a) Schematic of the SED device. The water splitting reactions take place on a platinum mesh electrode, similar to traditional electrodialysis. Water to be treated flows between two cation exchange membranes through a microporous borosilicate frit and is split into two streams by the splitter (black). (b) Photographs of a working device without the splitter attached (left) and with the splitter attached (right). Direction of flow is indicated by the blue arrow. (c) Experiment setup. Peristaltic pumps draw water from one of two feed tanks, pump through an accumulator and into the SED device for treatment. Samples are collected and analyzed for flow rate, pH, conductivity, and composition (using ICP-OES) [Color figure can be viewed at wileyonlinelibrary.com]

achieved five orders of magnitude reduction in copper sulfate concentration in two passes⁹ as well as disinfection and other separations.¹⁹ A scalable and continuous architecture was then developed and shown to achieve up to 99.99% ion removal in a single pass at up to 79% water recovery.⁷ Data collapse revealed that, for a variety of dilute binary electrolytes, the degree of desalination is only a function of the applied current scaled by the limiting current, which corresponds to incoming convective current of cations, given by $I_{lim} = z_+ c_+ F Q$, where z_+ and c_+ are the charge and total concentration of the salt cations, F is Faraday's constant, and Q is the inlet volumetric flow rate.⁷

In this article, we report the first study of continuous ionic separations from multicomponent electrolytes by SED, in the case of magnesium sodium chloride solutions. By systematically analyzing all the input and output streams, magnesium is shown to be selectively removed from the fresh stream, as a result of selective super-diffusive ion transport in the depleted region behind the shock within a porous glass frit. High selectivity also enables high water recovery and low energy cost, as the current is mostly carried by the target ions.

2 | MATERIALS AND METHODS

The experiments are performed on a similar prototype as the original scalable and continuous SED system,⁷ as shown in Figure 1b. The device requires three inlet streams (two electrode flush streams and one feed stream) and produces four outlet streams (two electrode flush streams, one brine stream, and one fresh stream), which are supplied to the device by 1/8 in. Tygon[®] tubing through cast acrylic porting plates. Four 1/16 in. Viton[®] gaskets are used to seal the device and provide the channels for the electrode flushes. The electrodes comprise a platinum mesh (Alfa Aesar) and are connected to the Keithley[®] 2450 SourceMeter using titanium wires (Alfa Aesar). The deionization shockwave is produced by passing over-limiting current through a porous borosilicate glass frit (Adams & Chittenden Scientific Glass, ultrafine, pore size 0.9–1.4 μm , BET internal area 1.75 m^2/g , mass density 1.02 g/cm^3 , porosity 0.31, and dimensions 20 \times 10 \times 8 mm^3). The electrode channels are fluidically separated from the porous frit by two cation exchange membranes (Nafion N112), whose selective transport of cations triggers a deionization shockwave propagating away from the cathode. The splitter is made of cast acrylic and sealed against the frit by Gore[®] ePTFE gasket tape (0.01 in.). The location of the splitter is flexible with higher positions (toward the anode) causing higher water recovery and lower desalination for the same current and flow rates. Then, 316 stainless steel nuts, bolts, and washers were used to hold the layers of the device together.

The Na-Mg feed solutions contain varying ratios of NaCl and MgCl₂ with a constant 10 mM concentration of Cl⁻, in order to focus on selective ion separation, rather than total desalination. The corresponding inlet salt concentrations are 3.33:3.33 mM for NaCl:MgCl₂ = 1:1 (base case), 0.91:4.5 mM for 1:5, 7.14:1.43 mM for 5:1, and 8.18:0.91 mM for 9:1. The effluent concentrations for 1:1 will be shown to be up to a 5:1 ratio in the fresh outlet stream, so the 5:1 case can also be viewed as an

artificial “second pass” of the separation, although a true second pass would begin more dilute than the 10 mM chloride concentration studied here. We also study the opposite 1:5 ratio, to explore separation under conditions of magnesium abundance. We also consider 9:1, which corresponds to the relative abundances of sodium and magnesium in seawater,²⁰ albeit at lower overall salinity.

The anode flush stream composition is identical to the feed stream. The cathode stream composition is similar to the other two, but has 50 mM HCl added as an antiscalant to prevent any precipitation of magnesium hydroxides that would occur as a result of the hydrogen evolution reaction. The electrode stream flow rates are 0.4 ml/min, and the feed stream flow rate is 0.06 ml/min.

Figure 1c shows a schematic of the experimental workflow. The solutions are fed to the SED device by peristaltic pumps, whose pulsating flows are stabilized by passing through an accumulator before entering the SED device. After separations and passage through the device, all the effluent streams were collected and measured for volume, conductivity, pH, and sodium and magnesium concentrations by Inductively Coupled Plasma–Optical Emission Spectroscopy (ICP-OES), which allows accurate detection of all species, as evidenced by closing the mass balances, as shown below.

3 | RESULTS AND DISCUSSION

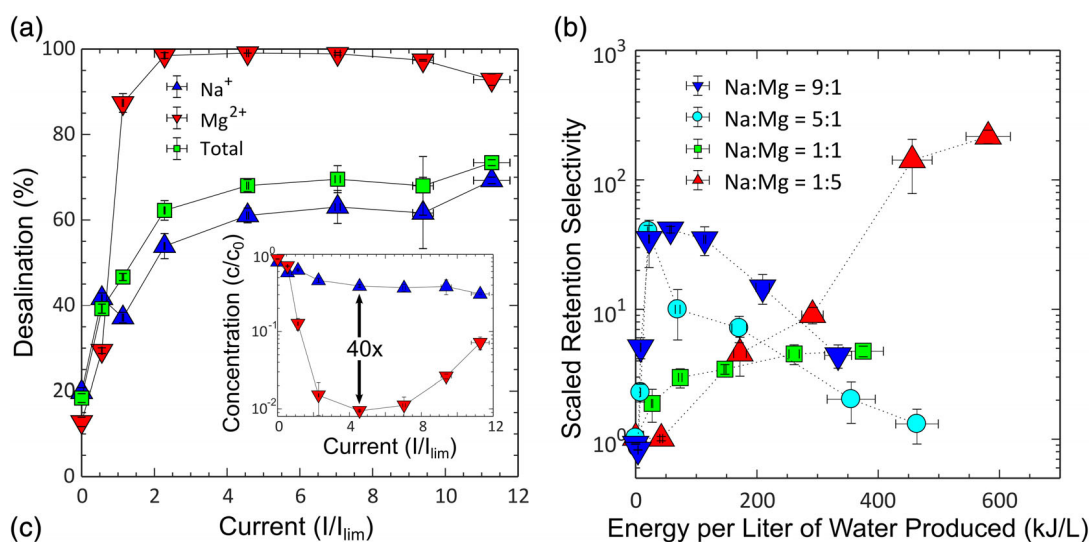
Figure 2a shows the ion-specific desalination performance ($Desalination = [1 - c_{i,out}/c_{i,feed}] \times 100\%$) for the 9:1 (“diluted seawater”)

feed condition. The magnesium removal peaks at a relatively low energy input and then decreases with increased energy. The sodium removal and total desalination increase with increased energy input, as expected, although the total desalination never reaches levels of complete deionization. The peak magnesium removal is $99.1 \pm 0.67\%$. At zero current, the apparent desalination is likely the result of H^+ from the cathode exchanging with Na^+ and Mg^{2+} across the membrane. Additional data and analysis for all four compositions studied is available in the Supporting Information.

The aggregated selectivities for each of the feed compositions studied are given in Figure 2b. The scaled retention selectivity for sodium versus magnesium can be thought of in one of two ways, either as the ratio of the effluent concentrations of sodium and magnesium, scaled by their ratio of inlet concentrations, or as the ratio of their scaled effluent concentrations:

$$\text{Scaled Retention Selectivity} = \frac{c_{Na}/c_{Mg}}{c_{Na,0}/c_{Mg,0}} = \frac{c_{Na}/c_{Na,0}}{c_{Mg}/c_{Mg,0}} \quad (1)$$

The trend in selectivity as a function of energy input changes dramatically with the changes in the inlet concentrations. For the system with the most magnesium, the selectivity monotonically increases with increased energy input. This is the case with the highest energy consumption, because of its low fresh-stream conductivity, resulting from high total desalination. The equimolar system also has a monotonically increasing selectivity with increased energy input, but the highest total selectivity is much lower than the other cases. For the



NaCl:MgCl ₂	Scaled Retention Selectivity	Total Desalination	Mg ²⁺ Removal	Current (I/I _{lim})	Energy (kJ/L)
9:1	41.3 ± 2.4	68.06 ± 1.41%	99.06 ± 0.02%	4.56 ± 0.03	57.5 ± 1.2
5:1	40.3 ± 4.2	56.27 ± 1.73%	98.59 ± 0.13%	1.96 ± 0.12	20.8 ± 1.1
1:1	4.75 ± 0.45	97.38 ± 0.40%	98.88 ± 0.24%	10.97 ± 0.66	375 ± 33
1:5	216 ± 26	98.70 ± 0.05%	99.94 ± 0.01%	10.54 ± 0.19	581 ± 37

FIGURE 2 (a) Desalination of Na^+ and Mg^{2+} and the relative retention of each species (inset) for an initial Na:Mg ratio of 9:1. All experiments performed in triplicate; error bars represent ± 1 SD. (b) The selective retention of ions across different feed compositions and energy input. (c) A table of the maximum-scaled retention selectivity, the total ion and target ion removal at that maximum for each feed composition, and the current and energy input required to achieve those selectivities and desalinations [Color figure can be viewed at wileyonlinelibrary.com]

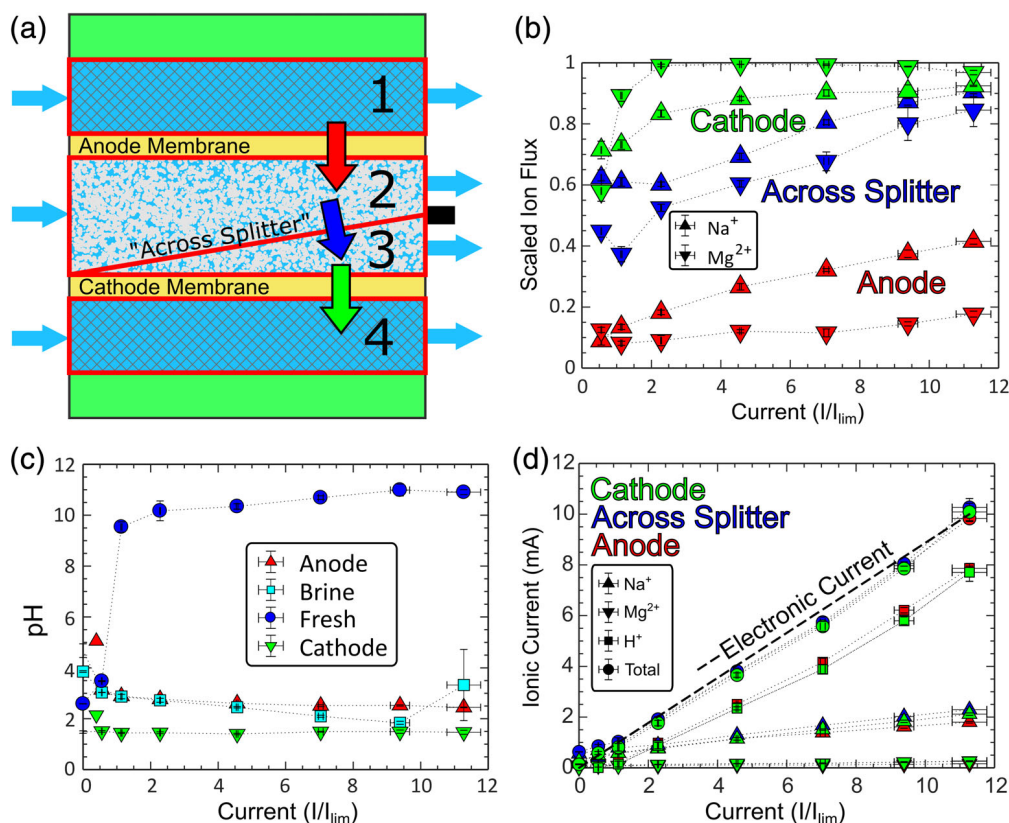


FIGURE 3 (a) Schematic showing control volumes (outlined in red) used for tracking current carriers (b) The fraction of ions crossing out of each control volume for an initial Na: Mg ratio of 9:1. (c) Effluent pH for each stream. (d) Closing the current balance. This is the total current carried out of each control volume by each cation. The dashed line represents the total applied electronic current [Color figure can be viewed at wileyonlinelibrary.com]

two cases of dilute magnesium in a stream dominated by sodium, the maximum selectivity comes at a low energy cost, which illustrates the possibility of highly efficient removal of trace multivalent ions from low salinity water. The effect of changing the total ion concentration on the selectivity is beyond the scope of this work, but we anticipate that increasing salinity may reduce overall ion selectivity, which arises mainly upon strong total salt depletion behind the shock. This effect is the subject of ongoing studies.

Figure 2c summarizes the best retention selectivity performance of the SED device at each feed composition. At maximum selectivity, the target ion removal is always over 98%, going as high as 99.94% in the case of a magnesium-rich feed. This impressive magnesium removal and scaled selectivity (>200) comes at a high-energy cost and requires very high total desalination to accomplish. Conversely, the case of $NaCl:MgCl_2 = 5:1$ can achieve over 98.5% removal of the target ion with only 56% total desalination. This low total desalination allows for a low current and high conductivity, giving an energy cost that is more than an order of magnitude lower than the energy cost in the 1:5 case. The overall energy consumption is higher than that of more established desalination technologies like RO^{21} or ED^{22} indicating that for the solutions studied, SED, in its early stage of development, may not be the preferred method of desalination. However, these results do show that as solutions become more dilute in the multivalent ion, the energy requirement drops. Though not studied here, SED may already hold promise in applications where the multivalent ion is (a) very dilute, (b) requiring complete elimination from solution,

and (c) in the presence of monovalent ions that do not need to be removed.

In an effort to understand the physical origins of selectivity in our SED system, the fluxes of all the ions in the system are calculated, closing the mass balances. Figure 3a is a schematic of the control volumes used to calculate the fluxes throughout the device, outlined in red and numbered as follows: 1 for the anode; 2 for brine, 3 for fresh, and 4 for the cathode. The light blue arrows represent ion fluxes in and out of the device, while color-coded, black-outlined arrows represent ion transport between control volumes. The choice made for control volumes 1 and 4 should be intuitive as they are fluidically separated from the other streams. The choice for how to separate control volumes 2 and 3 is less obvious. Ions in the feed enter into control volume 2. From there, they either exit the cell from control volume 2 or pass “across the splitter” into control volume 3. Of course, the fluid is not literally passing across the splitter, which is made of acrylic and positioned outside the control volumes. Instead, the line represents a flux that is approximately across the deionization shock. Calling it a flux “across the shock” would be misleading though, as the location of the shock changes based on the applied current and feed conditions. Unlike transport across the cation exchange membranes, transport across the splitter is not ion selective, and ions can be carried by advection as well as diffusion and electromigration.

The values of the fluxes into and out of the device are known from flow rates and measured concentrations. In order to calculate the values of ion fluxes perpendicular to flow, the following system of algebraic equations is solved:

$$\begin{aligned}
 N_{i,anode} &= c_{i,in,anode}q_{anode} - c_{i,out,anode}q_{anode} + R_i \\
 N_{i,splitter} &= c_{i,feed}q_{feed} + N_{i,anode} - c_{i,out,brine}q_{brine} \\
 N_{i,cathode} &= N_{i,splitter} - c_{i,out,fresh}q_{fresh}
 \end{aligned} \quad (2)$$

where N is the molar flow rate, c is the concentration, q is the volumetric flow rate, i refers to each of the three cations (Na^+ , Mg^{2+} , and H^+), and R_{H^+} is a reaction term for the production of H^+ by water splitting (all current is assumed to go to water splitting). The black-outlined arrow flux out of each control volume can be normalized by the total flux into that control volume:

$$\begin{aligned}
 \tilde{N}_{i,anode} &= \frac{N_{i,anode}}{c_{i,in,anode}q_{anode}} \\
 \tilde{N}_{i,splitter} &= \frac{N_{i,splitter}}{N_{i,anode} + c_{i,in,feed}q_{feed}} \\
 \tilde{N}_{i,cathode} &= \frac{N_{i,cathode}}{N_{i,splitter}}
 \end{aligned} \quad (3)$$

which makes the dimensionless ion flux (\tilde{N}_i) equivalent to the fraction of ions entering a control volume that leave the control volume across an interface (instead of leaving the device). As such, the dimensionless ion flux quantifies the ease with which a particular ion can cross a given interface, although it does not measure which ion carries the most current.

Figure 3b examines the scaled ion flux across each of the three interfaces for a feed with equimolar sodium and magnesium. As expected, the fraction of ions that are driven through the device increases with increased applied current. Transport across each membrane gives insight into the cause of the selectivity. Across the cathode membrane, corresponding to ions driven out of the fresh stream, the magnesium ions have a higher apparent mobility than sodium at $I \geq I_{lim}$. The opposite is true below I_{lim} . Sodium ions pass across the anode membrane more easily than magnesium. This is expected below limiting current, as sodium has a higher mobility than magnesium in Nafion,²³ and should be the case in the cathode membrane as well. Thus, magnesium is not being selectively shuttled by the membrane itself. Since the cathode membrane changes its selectivity with applied currents $I \geq I_{lim}$, a natural conclusion would be that the shock is primarily responsible for enhancing the magnesium transport out of the porous glass frit. This is unlike other continuous, selective separation technologies which rely on a selective surface to retain multivalent ions (e.g., nanofiltration²⁴ and selective membrane electrodialysis^{25,26}).

Analyzing transport within the frit also builds intuition about the mechanisms for selectivity. Across the splitter, sodium passes more easily. Sodium therefore passes (by advection and electromigration) more easily than magnesium through the brine region, but this reverses in the combined transport within the deionized region below the shock and across the cathode membrane. One possible mechanism for this change in apparent mobility is the divalent magnesium ions more closely associating with the negatively charged frit walls. In the brine region this slows their transport, while in the deionized region, this close proximity may become advantageous as SC and EOF dominate ion transport. The improved transport due to wall proximity may even be enough to offset the apparent selectivity for sodium transport of the cation exchange membranes.

The mechanism is also complicated by local changes in pH and their influence on surface charges of the membrane and glass frit. As a result, the membrane may behave differently when extreme deionization and large electric fields are present at its surface.²² In order to investigate these effects, the pH in each stream is plotted in Figure 3c. The increased pH in the deionized stream points to a water splitting reaction occurring at the membrane surface. This reaction could also play a role in the selective removal of magnesium, although the precise role of pH (if any) on the ion selectivity of SED merits further study to determine its impact on performance and specific applicability across use cases.

Conservation of charge implies that the total ionic current across each interface should be equal to the total applied electronic current. Figure 3d shows the breakdown of the current carriers, as well as the total current carried across each interface. As previously speculated,⁷ the majority of the current in the over-limiting regime is carried by H^+ , followed by Na^+ and Mg^{2+} , which carry amounts of current roughly proportional to their inlet charge concentrations. The total measured ionic current tracks closely with the total electric current applied to the system. Interestingly, at zero electronic current, the ionic current is nonzero. Across the cathode membrane, this is likely the result of ion exchange, as noted above. Because the concentration of negative ions is not explicitly measured, the advection of neutral salt across the splitter is misrepresented as a flux of only positive ions, leading to an overestimation of ionic current from region 2 to region 3.

In summary, our SED device is found to selectively remove magnesium from a mixture of NaCl and MgCl_2 . In the case with dilute Mg^{2+} , over 99% of Mg^{2+} is removed at a total desalination of only 68%, allowing the solution to maintain higher conductivity and in turn, consume less energy. Selectivity is shown to be the result of a large difference in ionic mobilities across the enriched and deionized regions of the device when overlimiting currents were applied. Specifically, sodium passes more easily across the anode membrane and through the frit, while magnesium passes more easily through the depleted region and through the cathode membrane for $I \geq I_{lim}$. Such complex phenomena of selective ion transport during deionization shock propagation, which have yet to be predicted theoretically, may find useful applications in municipal or industrial water treatment.


ACKNOWLEDGMENTS

This research was supported by the Massachusetts Institute of Technology-Tata Center for Technology and Design.

CONFLICT OF INTEREST

The authors declare no competing financial interest.

ORCID

Kameron M. Conforti  <https://orcid.org/0000-0002-0782-3048>
 Martin Z. Bazant  <https://orcid.org/0000-0002-8200-4501>

REFERENCES

1. WHO, UNICEF. Progress on drinking water, sanitation and hygiene. 2017. https://www.unicef.org/publications/files/Progress_on_Drinking_Water_Sanitation_and_Hygiene_2017.pdf. Accessed December 4, 2018.
2. Ganim S, Tran L. How tap water became toxic in Flint, Michigan. CNN. <http://www.cnn.com/2016/01/11/health/toxic-tap-water-flint-michigan/index.html>. Accessed February 29, 2016
3. Pieper KJ, Tang M. & Edwards, M. A. Flint water crisis caused by interrupted corrosion control: investigating 'ground zero' home. 2017. <https://pubs.acs.org/doi/abs/10.1021/acs.est.6b04034>. Accessed December 6, 2018
4. FlintWaterStudy.org. [Complete Dataset] Lead results from tap water sampling in flint, MI during the flint water crisis. Flint Water Study Updates. 2015.
5. Bazant MZ, Dydek EV, Deng D, Mani A. Method and apparatus for desalination and purification. US 8801910 B2, United States patent and trademark office. 2014.
6. Bazant MZ, Dydek EV, Deng D, Mani A. Desalination and purification system. US 8999132 B2, United States patent and trademark office. 2015.
7. Schlumpberger S, Lu NB, Suss ME, Bazant MZ. Scalable and continuous water deionization by shock Electrodialysis. *Environ Sci Technol Lett*. 2015;2:367-372.
8. Mani A, Bazant MZ. Deionization shocks in microstructures. *Phys Rev E*. 2011;84:061504.
9. Deng D, Dydek EV, Han JH, et al. Overlimiting current and shock Electrodialysis in porous media. *Langmuir*. 2013;29:16167-16177.
10. Nikonenko VV, Kovalenko AV, Urtenov MK, et al. Desalination at overlimiting currents: state-of-the-art and perspectives. *Desalination*. 2014;342:85-106.
11. Dydek EV, Zaltzman B, Rubinstein I, Deng DS, Mani A, Bazant MZ. Overlimiting current in a microchannel. *Phys Rev Lett*. 2011;107:118301.
12. Nam S, Cho I, Heo J, et al. Experimental verification of Overlimiting current by surface conduction and electro-osmotic flow in microchannels. *Phys Rev Lett*. 2015;114:114501.
13. Mani A, Zangle TA, Santiago JG. On the propagation of concentration polarization from microchannel–Nanochannel interfaces part I: analytical model and characteristic analysis. *Langmuir*. 2009;25:3898-3908.
14. Zangle TA, Mani A, Santiago JG. On the propagation of concentration polarization from microchannel–Nanochannel interfaces part II: numerical and experimental study. *Langmuir*. 2009;25:3909-3916.
15. Wang YC, Stevens AL, Han J. Million-fold Preconcentration of proteins and peptides by Nanofluidic filter. *Anal Chem*. 2005;77:4293-4299.
16. Kim SJ, Ko SH, Kang KH, Han J. Direct seawater desalination by ion concentration polarization. *Nat Nanotechnol*. 2010;5:297-301.
17. Kim SJ, Ko SH, Kang KH, Han J. Direct seawater desalination by ion concentration polarization. *Nat Nanotechnol*. 2013;8:609-609.
18. Dydek EV, Bazant MZ. Nonlinear dynamics of ion concentration polarization in porous media: the leaky membrane model. *AIChE J*. 2013;59:3539-3555.
19. Deng D, Aouad W, Braff WA, Schlumpberger S, Suss ME, Bazant MZ. Water purification by shock electrodialysis: deionization, filtration, separation, and disinfection. *Desalination*. 2015;357:77-83.
20. Pilson MEQ. *An introduction to the chemistry of the sea*. UK: Prentice Hall; 1998.
21. Alghoul MA, Poovanaesvaran P, Sopian K, Sulaiman MY. Review of brackish water reverse osmosis (BWRO) system designs. *Renew Sustain Energy Rev*. 2009;13:2661-2667.
22. Wright NC, Winter AG. Justification for community-scale photovoltaic-powered electrodialysis desalination systems for inland rural villages in India. *Desalination*. 2014;352:82-91.
23. Okada T, Xie G, Gorseth O, Kjelstrup S, Nakamura N, Arimura T. Ion and water transport characteristics of Nafion membranes as electrolytes. *Electrochim Acta*. 1998;43:3741-3747.
24. Mohammad AW, Teow YH, Ang WL, Chung YT, Oatley-Radcliffe DL, Hilal N. Nanofiltration membranes review: recent advances and future prospects. *Desalination*. 2015;356:226-254.
25. Luo T, Abdu S, Wessling M. Selectivity of ion exchange membranes: a review. *J Membr Sci*. 2018;555:429-454.
26. Giorno L, Drioli E, Strathmann H. Permselectivity of ion-exchange membranes. In: Drioli E, Giorno L, eds. *Encyclopedia of membranes*. Berlin: Heidelberg: Springer; 2016:1490-1493.

SUPPORTING INFORMATION

Additional supporting information may be found online in the Supporting Information section at the end of this article.

How to cite this article: Conforti KM, Bazant MZ. Continuous ion-selective separations by shock electrodialysis. *AIChE J*. 2019;e16751. <https://doi.org/10.1002/aic.16751>